東北大学機関リポジトリ
TOUR
Tohoku University Repository

東北大学

Magnetic Phase Stability and Spin-Dependent Transport in CeNi4M(M=Sc, Ti, V, Cr, Mn, Fe, and Co): First-Principles Study

	Murugan P., Bahramy M. S., Kawazoe Y.
journal or publication title	Physical Review B
volume	77
number	6
page range	064401
year	2008
URL	http://hdl.handle.net/10097/53188

doi: 10.1103/PhysRevB.77.064401

Magnetic phase stability and spin-dependent transport in CeNi$_4$M (M=Sc, Ti, V, Cr, Mn, Fe, and Co): First-principles study

P. Murugan,[*] M. S. Bahramy, and Y. Kawazoe

Institute for Materials Research, Tohoku University, Sendai, 980-8577, Japan

Using first-principles density functional calculations, the structural, magnetic, and spin-dependent transport properties of a set of intermetallic compounds CeNi$_4$M (M=Sc-Co) are investigated. All the compounds are considered to be in the orthorhombic phase, in which a transition metal atom M substitutes for one of the Ni atoms in the parent hexagonal CeNi$_5$ structure. The optimized lattice constants are shown to be in good agreement with the corresponding experimental data. The volume of CeNi$_4$M turns out to decrease with changing the M component from Sc to Co. Our calculations reveal that the ferromagnetic state is energetically more favorable for the compounds with M=Sc, Mn, Fe, and Co, while for CeNi$_4$Cr, the structure is found to be antiferromagnetic. Except for CeNi$_4$Sc, the magnetism in these compounds originates mainly from M atoms. The ferromagnetic coupling is mediated through the indirect d-d and d-f exchange interactions. The spin-dependent transport calculations show that the spin polarization in the diffusive regime is significantly higher than that in the ballistic one for these intermetallic compounds.

　　　　　　PACS number(s): 75.25.+z, 75.50.Cc, 71.20.Lp

I. INTRODUCTION

The intermetallic compound CeNi$_5$ is a well-known Pauli paramagnet, having a rich variety of physiochemical properties.[1] The compound is described as an intermediate valence system, as it exhibits anomalous values of lattice constants in RNi$_5$ (R=rare earth elements) series.[2,3] Alongside, CeNi$_5$ yields a relatively large Stoner exchange-enhancement factor ($\sim$4.0) with a maximal magnetic susceptibility at around 100 K, typical for nearly ferromagnetic systems.[3] As a consequence, the compound has the capability of becoming ferromagnetic either by applying a relatively large magnetic field[4] or by introducing 3d transition metal (TM) atoms such as Mn or Fe.[5] In the latter, the net magnetic moment turns out to be substantially large with dominant contributions from TM 3d states. In the particular case of CeNi$_4$Mn, the recent point contact Andreev reflection[6] measurements have interestingly shown the compound to have also a relatively large spin polarization value ($\sim$66%) at 2.8 K (Ref. 7) and, thereby, to be potentially a promising material for spintronics applications. Surprisingly, the further theoretical studies based on the local spin density (LSDA) and LSDA+U approximations reveal a much lower degree of spin polarization in CeNi$_4$Mn, varying from $-$22 to 10%.[8–11] In explanation, the possibility of the formation of structural defects or chemical disorders in the experimentally prepared CeNi$_4$Mn samples has been suspected to be the reason for this discrepancy.[9,11]

Structurally, CeNi$_5$ and most of its related TM doped alloys CeNi$_{5-x}$M$_x$ (M=TM atom) crystallize in the hexagonal structure.[5,12,13] The only exception is CeNi$_{5-x}$Mn$_x$ for which cubic structures are experimentally found to be more stable for TM concentrations x=0.9$-$2.1.[14] However, here again the LSDA-based calculations on CeNi$_4$Mn disobey the experiment.[10] Theoretically, CeNi$_4$Mn and other CeNi$_4$M compounds are expected to be stabilized in a hexagonal structure with the space group of *Cmmm*, which is geometrically lower in symmetry as compared with the parent hex-

agonal structure CeNi$_5$ (with the $P6/mmm$ space group). Thus, CeNi$_4$M can be somewhat described as an orthorhombic compound (as will be discussed later).

As regards the magnetism and spin-dependent transport, the CeNi$_4$M compounds have not been yet well studied. In fact, we have only little information about the magnetic and spin-dependent properties of CeNi$_4$Mn and CeNi$_4$Fe.[5,7] In this paper, we present a detailed and systematic first-principles study in order to understand such properties of CeNi$_4$M compounds. For this purpose, various 3d-TM atoms (Sc, Ti, V, Cr, Mn, Fe, and Co) are considered for the M component. As experimentally observed for CeNi$_4$Mn and CeNi$_4$Fe,[5] we show that these two structure as well as CeNi$_4$Sc and CeNi$_4$Co are ferromagnetic whereas CeNi$_4$Cr and finally CeNi$_4$Ti and CeNi$_4$V are antiferromagnetic and nonmagnetic in their ground-state configurations, respectively. As regards to the spin-dependent transport, the calculations reveal a higher degree of spin polarization in the diffusive regime rather than in the ballistic one. Finally the effect of structural disorders in spin-transport is discussed in terms of the small shifts in the Fermi energy of the compounds.

II. COMPUTATIONAL METHODS

In this work, the calculations are carried out within the context of the density functional theory (DFT) using the gradient-corrected PW91 exchange-correlation functional[15] and the projected augmented wave (PAW) method,[16] as implemented in the VASP code.[17] To simulate both ferromagnetic (FM) and antiferromagnetic (AFM) alignments in each CeNi$_4$M compound, we consider an orthorhombic unit cell, containing 2 Ce, 8 Ni, and 2 M atoms. The corresponding Brillouin zone (BZ) is sampled by a $4\times6\times8$ Monkhorst-Pack[18] (MP) mesh. Using the conjugate gradient method, the full structural optimization is performed for all configurations until the magnitude of the force is less than 0.005 eV/Å on each atom. For AFM calculations we con-

sider two different magnetic configurations. In the first configuration, the M atoms are antiferromagnetically aligned along the kagome lattice. For the second one, the M atoms in the same kagome lattice are ferromagnetically aligned, whereas they are antiferromagnetically ordered in respect to the next consecutively repeated kagome interlayer. For the sake of simplicity, throughout this work, the two configurations are denoted as xy-AFM and z-AFM, respectively. In the latter, a $1 \times 1 \times 2$ supercell (similar to the above orthorhombic cell but twice as large as that along the z axis) is constructed. Correspondingly, the new Brillouin zone is sampled by a $4 \times 6 \times 4$ MP mesh. As the total energy values E^{total} are obtained for FM and both xy-AFM and z-AFM configurations, the corresponding in-plane and perpendicular total energy differences ΔE_{xy} and ΔE_z, respectively, are computed with

$$\Delta E_{xy} = E_{\text{FM}}^{\text{total}} - E_{xy\text{-AFM}}^{\text{total}}, \tag{1}$$

$$\Delta E_z = E_{\text{FM}}^{\text{total}} - E_{z\text{-AFM}}^{\text{total}}. \tag{2}$$

These two quantities are then used to describe the relative magnetic stability and, accordingly, the exchange interaction in each CeNi$_4$$M$ compound.[19–21]

For FM systems, the degree of spin polarization, P, are evaluated in both ballistic and diffusive regimes, following the Mazin's approach in which P is defined as[22]

$$P_n = \frac{\langle N v_F^n \rangle_\uparrow - \langle N v_F^n \rangle_\downarrow}{\langle N v_F^n \rangle_\uparrow + \langle N v_F^n \rangle_\downarrow}, \tag{3}$$

where N and v_F are the density of state at Fermi energy ε_F and the Fermi velocity of electrons with spin σ ($\uparrow$ and $\downarrow$), respectively. The index n indicates the static (P_0), ballistic (P_1), and diffusive (P_2) limits. It is worth mentioning that in the transport experiments, such as PCAR, one can probe the degree of spin polarization in either ballistic or diffusive regimes, depending on the characteristic size of the contact d and the mean free path of the electrons, l in the system. If d is smaller than l, the electrons flow through the contact ballistically. In the opposite case, when $d \gg l$, they perform a diffusive motion. It is to be noted that, within the Mazin's approach, the state-dependent transmittance of the barrier
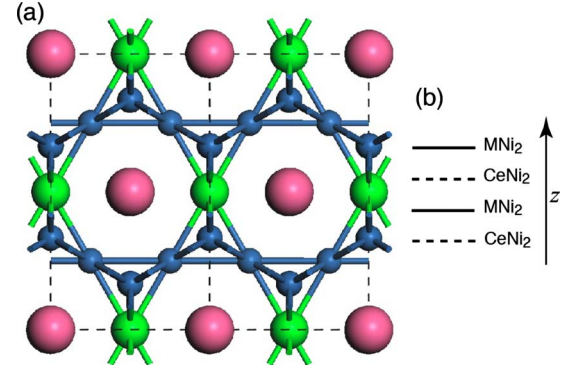

FIG. 1. (Color online) (a) The side view of the crystal structure of orthorhombic CeNi$_4$$M$ compounds along the z axis and (b) illustrative diagram for the layer arrangements along the z axis of the compound. Ce, Ni, and M atoms are indicated as large (pink), small (blue), and medium (green) balls, respectively.

and contact is neglected.[22] The Fermi surface integration in Eq. (3) are carried out using our tetrahedron-based approach, as proposed in Ref. 11.

III. RESULTS AND DISCUSSIONS

A. Structural properties of CeNi$_4$$M$

The structure of CeNi$_4$$M$ compounds can be derived from CeNi$_5$, a well-known hexagonal CaCu$_5$ structure. The parent compound crystallizes in $P6/mmm$ group (No. 191), in which Ni atoms occupy both $2c$ (2/3, 1/3, 0) and $3g$ (1/2, 1/2, 1/2) sites and Ce is in the origin (0, 0, 0). In CeNi$_4$$M$, the substitutional M atom prefers any of $3g$ Ni sites, rather than $2c$ site (see CeNi$_4$Ga in Ref. 23). As a result, the derived structure reduces to an orthorhombic symmetry with the space group of $Cmmm$ (No. 65), as depicted in Fig. 1. In this structure, the two layers, MNi$_2$ and CeNi$_2$ are consecutively repeated along the z axis. The former creates a kagome lattice, whereas in the latter, Ce atoms are surrounded by six hexagonally arranged $2c$ Ni atoms.

Table I summarizes the lattice constants for CeNi$_4$$M$ (M = Sc-Co) as obtained from our structural optimization calcu-

TABLE I. Comparison of the lattice parameters (in Å) and the corresponding volume (in Å^3) of the CeNi$_4$$M$ compounds.

M	Present work				Experiment			
	a_H	b_H	c_H	V	a_H	c_H	V	Ref.
Sc	5.03	5.13	4.19	93.58				
Ti	4.87	5.15	4.11	89.28				
V	4.77	5.17	4.05	86.52				
Cr	4.88	5.03	4.06	85.77	4.905	4.019	83.74	12
Mn	4.87	5.02	4.05	85.59	4.921	4.054	85.02	5[a]
Fe	4.81	5.04	4.02	84.58	4.927	4.038	84.90	5
Co	4.88	4.91	3.99	82.79	4.895	3.998	82.94	13

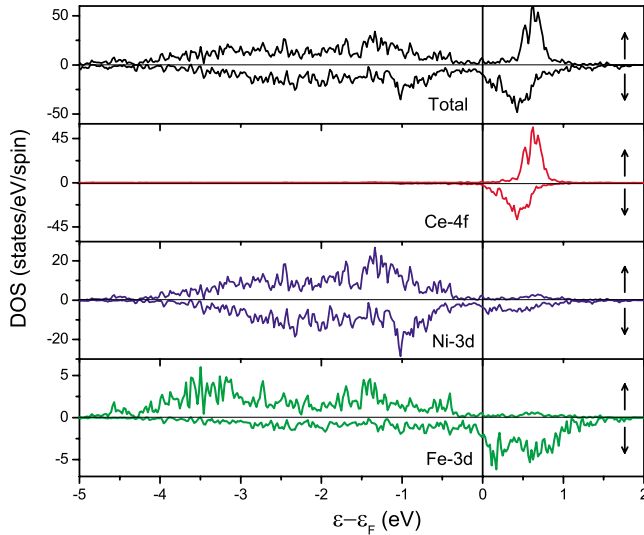[a]Experimental values for CeNi$_{4.25}$Mn$_{0.75}$.

FIG. 2. (Color online) The spin-polarized total and partial density of states for CeNi$_4$Fe. The majority and minority states are denoted by up and down arrows, respectively.

lations and as experimentally reported in the literature (wherever available). For a better comparison, the calculated orthorhombic lattice constants (a, b, c) are transformed to a hexagonal coordinate system ($\gamma = 120°$) within which the new lattice constants are $a_H = a/\sqrt{3}$, $b_H = b$, and $c_H = c$. The table clearly indicates an excellent agreement between the calculated c_H values with the corresponding experimental data. The other two calculated lattice constants a_H and b_H slightly differ from the experimental a_H value, such that the latter always lies between the two calculated a_H and b_H values. However, such differences are small and still less than 2.5% (for CeNi$_4$Fe). The volume of the CeNi$_4$M unit cells turns out to decrease as the substitutional component M changes from Sc to Co. This can be attributed to a similar decrease in the atomic radius of M from Sc to Co. In these intermetallic compounds, the Ce-Ni and Ni-M bond distances are around 2.8 and 2.5–2.4 Å, respectively, while the Ce-M bond distance varies from 3.31 Å (for M=Sc) to 3.16 Å (M=Co).

B. Electronic and magnetic properties

As a first step to understand the electronic and magnetic properties of CeNi$_4$M compounds, the electronic structure

calculations are carried out for CeNi$_4$Fe. The respective total and partial density of states (DOS) are shown in Fig. 2. The figure clearly indicates that, for both spin channels, the Ni-3d states are nearly fully occupied, whereas the Ce-4f states are almost unoccupied. In the latter, however, there is a slight shift between the spin-up and spin-down states, which can be attributed to the exchange interaction of the spin-down Fe-3d states with the corresponding Ce-4f levels. The figure also indicates that the magnetism in CeNi$_4$Fe originates mainly from Fe atoms. This is due to a large exchange splitting between the spin-up and spin-down Fe-3d states so that, the former are fully occupied and deeply located below ε_F, while the latter are only partially occupied. Such a large exchange splitting results in a dominant localization of the magnetic moment on the Fe atoms with a subsequently induced moments on the Ce and Ni atoms.

Table II summarizes the total and local magnetic moments for CeNi$_4$Fe as well as the other CeNi$_4$M compounds except for CeNi$_4$Ti and CeNi$_4$V. For these two compounds, our calculations reveal a nonmagnetic ground-state configuration in which the magnetic moments on M as well as the Ce and Ni atoms are negligibly small (nearly zero). Interestingly, for CeNi$_4$Sc the magnetic moment is obtained to be mainly because of Ce atoms ($\sim 0.23 \mu_B$/atom) with almost no contribution from the Sc and Ni sites. With this exception, the M atoms turn out to contribute dominantly to the total magnetic moments in the CeNi$_4$M compounds. The largest total magnetic moment is obtained for CeNi$_4$Mn (3.73μ_B/f.u.) with the respective local moments (in μ_B/atom) -0.46, 2.93, 0.29, and 0.37 on Ce, Mn, Ni-2g, and Ni-3c atoms.

Our calculations reveal that the induced moments on Ce(Ni) atoms have an opposite (similar) sign in respect to the magnetic moment of M atoms. This is in fact in agreement with the experimental findings for CeNi$_4$Fe.[5] A more detailed analysis on the magnetic moments on the two different Ni sites Ni-3c and Ni-2g indicates that the local moment on the former is larger than that on Ni-2g sites. This is due to the fact that the kagome lattice formed by the M and Ni-3c atoms enhances the exchange interaction of M with the Ni atoms in the kagome plane, resulting in a more pronounced induction of the magnetic moment on the Ni-3c sites as compared with that on the Ni-2g sites.

To our knowledge, CeNi$_4$Mn and CeNi$_4$Fe are the only compounds out of the others, discussed here, whose magnetic properties have been experimentally studied.[5,7] For the latter, the total magnetic moment is observed to be

TABLE II. Magnetic properties of orthorhombic CeNi$_4$M compounds. The local and total magnetic moments and total energy differences ΔE_{xy} and ΔE_z are in μ_B/atom, μ_B/f.u., and eV, respectively.

| | Magnetic moments | | | | | | |
M	Ce	M	Ni-2g	Ni-3c	total	ΔE_{xy}	ΔE_z
Sc	0.23	0.02	0.00	0.00	0.38	0.01	0.01
Cr	0.07	2.16	0.14	0.15	3.00	0.13	-0.07
Mn	-0.46	2.93	0.29	0.37	3.73	0.26	0.02
Fe	-0.55	2.48	0.34	0.44	3.33	0.18	0.20
Co	-0.49	1.16	0.27	0.36	1.76	0.07	0.12

$\sim 3.3 \mu_B/$f.u. with the local moment $\sim 0.4 \mu_B/$atom induced on each Ni atoms. It is to be noted that, the experimental measurements of Ni local moments are based on the assumption that the Ce atoms in CeNi$_4$Fe have no magnetic moment.[5] Nevertheless, the calculated total magnetic moment, $\sim 3.3 \mu_B/$f.u., is in excellent agreement with the experiment. Also, the local magnetic moments, calculated for Ni atoms in both Ni-2g ($\sim 0.34 \mu_B/$atom) and Ni-3c ($\sim 0.44 \mu_B/$atom), agree well with the corresponding experimental data.

As mentioned earlier, there is a structural phase transition from hexagonal to cubic phase around $x=0.9$ in CeNi$_{5-x}$Mn$_x$.[14] The saturation magnetic moment for the hexagonal CeNi$_{4.25}$Mn$_{0.75}$ is experimentally observed to be $\sim 0.38 \pm 0.02 \mu_B/$f.u.[5] However, our calculated magnetic moment is $3.73 \mu_B/$f.u. for $x=1.0$, which is quite larger than that observed for $x=0.75$. Hence, there could be a possibility of the magnetic phase transition in x varying from 0.75 to 1.0, leading to a significant increase in the magnetic moment of Mn atoms.

To further understand the magnetic stability in the CeNi$_4M$ compounds, we next consider the two different antiferromagnetic configurations xy-AFM and z-AFM described in Sec. II. The in-plane (perpendicular) total energy differences ΔE_{xy} (ΔE_z) are then calculated using Eqs. (1) and (2). The respective values are summarized in Table II. As shown, ΔE_z is negative for CeNi$_4$Cr. It indicates that this compound in its ground state stabilizes in an AFM state. As a result, the net magnetic moment becomes zero, however, one can still find some moments along the kagome lattice. For $M=$Mn, Fe, and Co, both ΔE_{xy} and ΔE_z are positive. The small energy differences are obtained for CeNi$_4$Sc compound. It is understandable, because of the fact that here the magnetic moments is mainly localized on Ce atoms (see Table II).

To find out the origin of the exchange interaction in CeNi$_4M$ compounds, we have illustrated in Fig. 3, the differential charge density $\delta\rho=\rho_{\text{FM}}-\rho_{xy\text{-AFM}}$ for CeNi$_4$Fe, as an example. The figure clearly shows a strong $(f\text{-}d)$-like charge distribution among the Fe and Ni atoms in the kagome lattice. This in turn implies that, the FM alignment on the Fe atoms is mainly mediated through indirect $d\text{-}d$ and $d\text{-}f$ exchange interactions. To be more precise, the indirect exchange interactions are expected to dominate the FM couplings between the Fe atoms. The simplest explanation[24] is that, since the angle $\angle$Fe-Ni-Fe made by Fe and Ni atoms in the kagome lattice is equal with 180°, there is almost no chance for two Fe atoms in the kagome lattice to directly interact with each other. Instead, the FM coupling between them comes from an indirect exchange interaction mediated by the central Ni atom. Along the z axis, where the Fe atoms in adjacent kagome layers are separated by the CeNi$_2$ layer (see Fig. 1), the FM coupling between Fe atoms is still expected to be dominantly mediated through indirect $d\text{-}d$ ($d\text{-}f$) exchange interaction induced between Fe and Ni(Ce) atoms.

C. Spin-dependent transport properties

Using Eq. (3), we next calculate the spin polarization P_n ($n=0-2$) for CeNi$_4M$ ($M=$Cr, Mn, Fe, Co) in order to un-
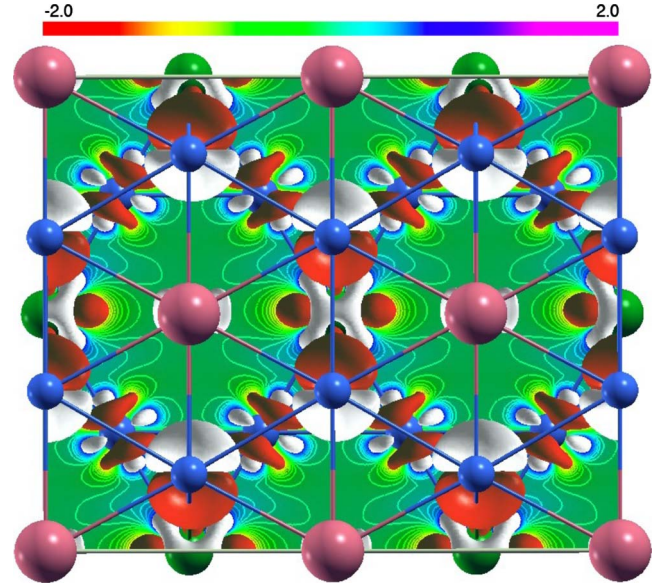

FIG. 3. (Color online) The isosurface and contour plots of the differential charge density $\delta\rho=\rho_{\text{FM}}-\rho_{xy\text{-AFM}}$ for CeNi$_4$Fe. The respective values of charge density for the light-colored (white) and dark-colored (red) isosurfaces are -0.8 and $+0.8$ (e/Å^3). Ce, Ni, and Fe atoms are indicated as large (pink), small (blue), and medium (green) balls, respectively.

derstand their spin-related transport properties. Table III summarizes the calculated P_n values as well as the averaged Fermi velocities $\langle v_\uparrow \rangle$ and $\langle v_\downarrow \rangle$ in respective spin-up and spin-down channels. An overall comparison between the P_n values reveals that, for all the compounds, P_0 and P_2 are comparable in magnitude (except for CeNi$_4$Mn) but opposite in sign (the reason for this sign difference will be explained later). Additionally, P_1 has a moderate value so that it lies between the corresponding P_0 and P_2 values for all the compounds. The only exception is CeNi$_4$Cr in which P_1 is slightly larger than P_2. Nevertheless, the calculated spin polarization in both ballistic and diffusive limits as well as the static one is very low (less than 8%) for this compound. Accordingly, the orthorhombic CeNi$_4$Cr is expected to exhibit very poor spin-transport properties.

To further analyze the spin polarization results, shown in Table III, we have calculated the spin polarized total- and s-projector DOS of the above CeNi$_4M$ compounds. The re-

TABLE III. Comparison of spin polarization P_n values (in %) for CeNi$_4M$ compounds. The table also includes the calculated averaged Fermi velocities $\langle v_F \rangle$ in both spin channels (in 10^5 m/s).

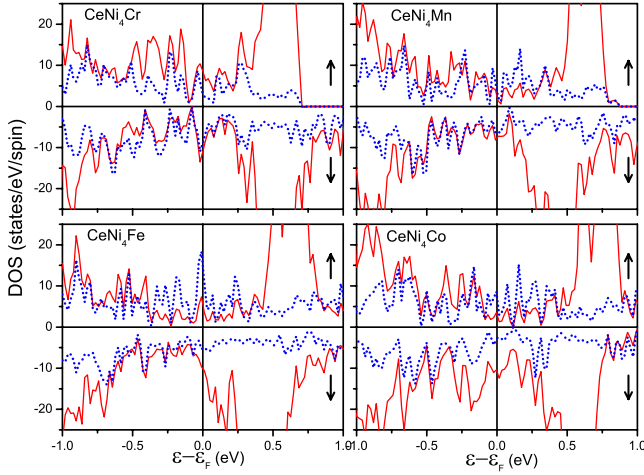| M	Polarization			Fermi velocity	
	P_0	P_1	P_2	$\langle v_F \rangle_\uparrow$	$\langle v_F \rangle_\downarrow$
Cr	−5.7	7.3	6.4	1.10	0.85
Mn	−46.7	−19.7	5.2	1.98	1.07
Fe	−48.6	−5.0	46.6	1.91	0.73
Co	−62.8	−12.4	43.9	2.57	0.75

FIG. 4. (Color online) Spin-polarized total and s-projected density of states for CeNi$_4$M (M=Cr, Mn, Fe, and Co). The respective total and s-projected DOS are indicated by solid and dotted lines. The latter is scaled up by 50.

FIG. 5. (Color online) Dependence of the degree of spin polarization P_n (n=0, 1, and 2) to the shift in energy ε for various CeNi$_4$M compounds.

spective DOS diagrams are illustrated in Fig. 4. Evidently, all the compounds at ε_F represent a relatively larger total-DOS value in spin-down channel $N_\downarrow$ than that in spin-up channel $N_\uparrow$. This explains why the calculated P_0 values have negative sign (see Table III). It is to be noted that, both $N_\uparrow$ and $N_\downarrow$ are substantially dominated by the transition metals $3d$ states (see, for example, Fig. 2). Thus, the obtained static spin polarization P_0 is expected to be mainly due to the spin splitting of TM $3d$ states at ε_F.

Similar to P_0, the spin polarization in both ballistic and diffusive regimes depends on $N_\uparrow$ and $N_\downarrow$ values. However, here, unlike in P_0, the type of the Fermi electrons plays a crucial role, also. This point is reflected in Eq. (3) by introducing the weighting factors v_F and v_F^2 for P_1 and P_2, respectively. From the electronic structure point of view, Fermi electrons with s character have the highest v_F among the other type of carriers and, hence, they contribute substantially to the transport.[11] On the other hand, the d and f electrons at ε_F have a small impact on the transport current due to their large effective mass and, consequently, low v_F. As a result, the P_n values are expected to differ considerably from each other, if there is a considerable imbalance between the averaged number of spin-up and spin-down Fermi s electrons. Returning to Fig. 4, one immediately notices that, in CeNi$_4$Mn, CeNi$_4$Fe, and CeNi$_4$Co, the value of spin-up s-DOS at ε_F, $N_\uparrow^s$, is significantly larger than the corresponding $N_\downarrow^s$ value, while $N_\uparrow \ll N_\downarrow$. Thus, the averaged values of spin-up Fermi velocity $\langle v_F \rangle_\uparrow$ turn out to be significantly larger than the corresponding $\langle v_F \rangle_\downarrow$ values (see Table III). Even in the case of CeNi$_4$Cr for which $N_\uparrow^s < N_\downarrow^s$, $\langle v_F \rangle_\uparrow$ is obtained to be still slightly larger than $\langle v_F \rangle_\downarrow$. This is because of the fact that, here again $N_\uparrow \ll N_\downarrow$ so that the averaged number of Fermi s electrons in spin-up channel becomes comparatively larger than that in spin-down channel. Consequently, for all these compounds, there is a noticeable difference between the obtained P_n values. Such a difference is so
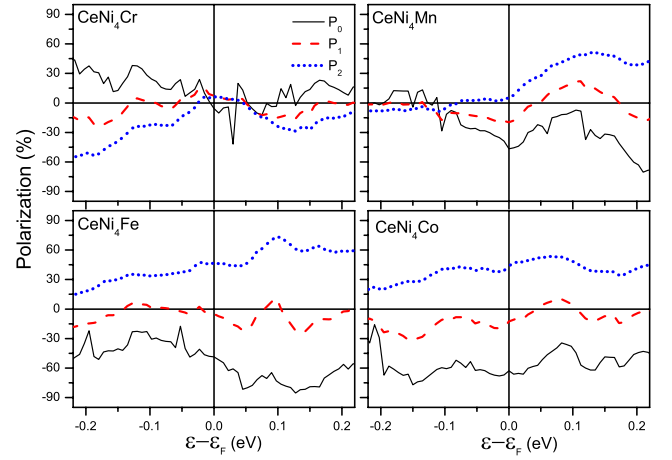
qualitatively significant that the sign of the corresponding P_2 values becomes positive, as indicated in Table III.

As there is a possibility of the formation of defects or chemical disorders in the experimentally prepared CeNi$_4$M samples, we further study the effect of such structural impurities on spin polarization in various regimes. In this regard, P_n (n=0, 1, and 2) values are calculated for CeNi$_4$M (M=Cr, Mn, Fe, Co) in an energy range of $\varepsilon_F \pm 0.2$ eV, assuming a rigid electronic band structure for all these compounds. The respective diagrams of P_n dependence to the ε shifts are depicted in Fig. 5. For CeNi$_4$Cr, the magnitude of P_n values are more or less increased by lowering the Fermi energy. This can be experimentally achieved by adding small amounts of Cr into the compound. In contrast, a different trend of spin polarization is obtained for CeNi$_4$Mn and CeNi$_4$Fe. Here P_0 with some oscillations and P_2 steadily are enhanced by removal of small amount of Mn. Interestingly, the slight addition or removal of Co atoms turn out to have almost no effect on the corresponding P_n values for CeNi$_4$Co. Despite the mentioned differences, Fig. 5 reveals a striking similarity in the trend of spin polarization in the above compounds. That is, shifting ε_F in this range of energy, the spin polarization in diffusive regime still tends to be substantially larger than that in ballistic regime. Experimentally speaking, it means that, for all these compounds the spin-dependent transport is expected to be more effectively achieved with a diffusive contact rather than the ballistic one.

IV. CONCLUSION

Within the generalized gradient approximation, the structural, magnetic, and the spin-dependent transport properties were studied for the orthorhombic phase of CeNi$_4$M (M=Sc-Co) intermetallic compounds. The calculated lattice constants and magnetic moments turned out to be in good agreement with available experimental data. For CeNi$_4$M

with $M=$ Sc, Cr, Mn, Fe, and Co, the ground-state structure were FM, while for the rest of compounds, it was found to be NM ($CeNi_4Ti$ and $CeNi_4V$) or AFM ($CeNi_4Cr$). The magnetism originated mainly from the M atoms, in all the compounds except for $CeNi_4Sc$. Moreover, the FM alignments among the M atoms was shown to be mainly because of indirect d-f and d-d exchange interactions. Our spin-polarization calculations revealed that the diffusive spin transport was substantially higher than the ballistic one. In this regard, the orthorhombic $CeNi_4Fe$ and $CeNi_4Co$ compounds were predicted to exhibit the most pronounced spin-dependent transport properties among the other compounds of this family.

*Present address: Central Electrochemical Research Institute, Karaikudi - 630006, Tamil Nadu, India.

[1] K. H. J. Buschow, Rep. Prog. Phys. **40**, 1179 (1977).

[2] U. Gottwick, K. Gloos, S. Horn, F. Steglich, and N. Grewe, J. Magn. Magn. Mater. **47&48**, 536 (1985).

[3] L. Nordstrom, M. S. S. Brooks, and B. Johansson, Phys. Rev. B **46**, 3458 (1992).

[4] D. Gignoux, F. Givord, R. Lemaire, and F. Tasset, J. Magn. Magn. Mater. **50**, 53 (1985).

[5] F. Pourarian, M. Z. Liu, B. Z. Lu, M. Q. Huang, and W. E. Wallace, J. Solid State Chem. **65**, 111 (1986).

[6] A. F. Andreev, Zh. Eksp. Teor. Fiz. **46**, 1823 (1964) [Sov. Phys. JETP **19**, 1228 (1964)].

[7] S. Singh, G. Sheet, P. Raychaudhuri, and S. K. Dhar, Appl. Phys. Lett. **88**, 022506 (2006).

[8] I. I. Mazin, Phys. Rev. B **73**, 012415 (2006).

[9] E. N. Voloshina, Y. S. Dedkov, M. Richter, and P. Zahn, Phys. Rev. B **73**, 144412 (2006).

[10] P. Murugan, A. K. Singh, G. P. Das, and Y. Kawazoe, Appl. Phys. Lett. **89**, 222502 (2006).

[11] M. S. Bahramy, P. Murugan, G. P. Das, and Y. Kawazoe, Phys. Rev. B **75**, 054404 (2007).

[12] R. K. Jain, A. Jain, S. Agarwal, N. P. Lalla, V. Ganesan, D. M. Phase, and I. P. Jain, J. Alloys Compd. **430**, 165 (2007).

[13] S. N. Klyamkin, N. S. Zakharkina, and A. A. Tsikhotskaya, J. Alloys Compd. **398**, 145 (2005).

[14] Y. M. Kalychak, O. I. Bodak, and E. I. Gladyshevskii, Izv. Akad. Nauk SSSR, Neorg. Mater. **12**, 1149 (1976) [Inorg. Mater. **12**, 961 (1976)].

[15] J. P. Perdew, J. A. Chevary, S. H. Vosko, K. A. Jackson, M. R. Pederson, D. J. Singh, and C. Fiolhais, Phys. Rev. B **46**, 6671 (1992).

[16] P. E. Blochl, Phys. Rev. B **50**, 17953 (1994).

[17] Vienna *Ab initio* Software Packages (VASP), version 4.6.12, http://cms.mpi.univie.ac.at/vasp/

[18] H. J. Monkhorst and D. J. Pack, Phys. Rev. B **13**, 5188 (1976).

[19] R. Hafner, D. Spišák, R. Lorenz, and J. Hafner, J. Appl. Phys. **87**, 5756 (2000).

[20] H. C. Herper, L. Szunyogh, P. Entel, and P. Weinberger, Phys. Rev. B **68**, 134421 (2003).

[21] C. Kittel, *Introduction to Solid State Physics*, 8th ed. (Wiley, New York, 2005).

[22] I. I. Mazin, Phys. Rev. Lett. **83**, 1427 (1999).

[23] H. Flandorfer, P. Rogl, K. Hiebl, E. Bauer, A. Lindbaum, E. Gratz, C. Godart, D. Gignoux, and D. Schmitt, Phys. Rev. B **50**, 15527 (1994).

[24] J. B. Goodenough, *Magnetism and Chemical Bond* (Interscience, New York, 1963).